Laboratory Investigation (2018) 98, 694–695

INSIDE THE USCAP JOURNALS

doi:10.1038/s41374-018-0059-z

MODERN PATHOLOGY

Hepatotoxicity with immune checkpoint inhibitors

doi:10.1038/s41379-018-0013-y

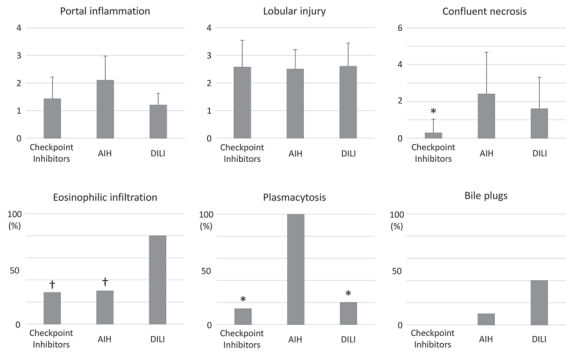

Zen and Yeh investigated the clinicopathologic features of both immune checkpoint inhibitor–induced liver injury and classic organ-specific autoimmune diseases such as autoimmune hepatitis and idiosyncratic drug-induced liver injury in order to assess the histologic and pathogenic features of these processes. Seven patients—five treated with nivolumab and two treated with ipilimumab—presented with elevated liver enzymes at a median of 41 days following the initiation of immunotherapy, which normalized following cessation of immunotherapy and/or addition of immunosuppression with corticosteroids. All biopsies showed predominantly lobular hepatitis with milder portal inflammation. The authors also looked at lymphocyte activation and found fewer $CD20^+$, $CD3^+$, $CD4^+$, or $CD8^+$ lymphocytes in checkpoint inhibitor-associated hepatitis than in autoimmune hepatitis. They note that, in contrast to what is commonly seen in autoimmune hepatitis, checkpoint inhibitor–induced liver injury can cause hepatocyte necrosis without activation of helper T cells and immunoglobulin production.

Heterogeneity in immunotherapy response signatures

doi:10.1038/s41379-018-0029-3

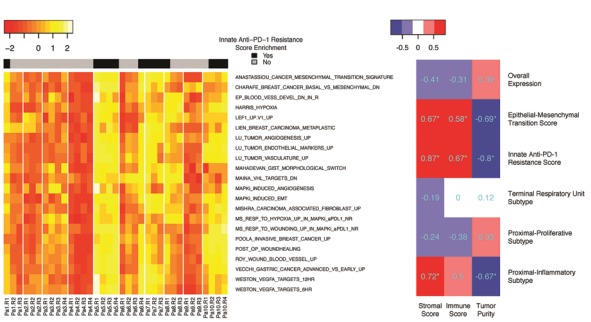

While genomic intratumor heterogeneity at the exome level has been reported in many cancer types, the details have not been well delineated in the context of immune checkpoint inhibitor therapy. By analyzing gene (RNA) expression profiles of 35 tumor regions from 10 non–small cell lung cancer tumors, Lee et al. found that intertumor heterogeneity was generally higher than intratumor heterogeneity, although some tumor types showed substantial intratumor heterogeneity. The changes observed in gene expression were associated with heterogeneous tumor microenvironments represented by stromal and immune cell infiltrates. The authors determined that caution should be exercised in using gene expression–based prognostic signatures from a single biopsy, which can either under- or overestimate the risk of recurrence of patients with non–small cell lung cancer due to the intratumor heterogeneity in gene expression. Intratumor heterogeneity should be taken into account if these gene expression–associated signatures are used as biomarkers.

LABORATORY INVESTIGATION

CRISPR reveals sorafenib target in HCC

doi:10.1038/s41374-018-0027-6

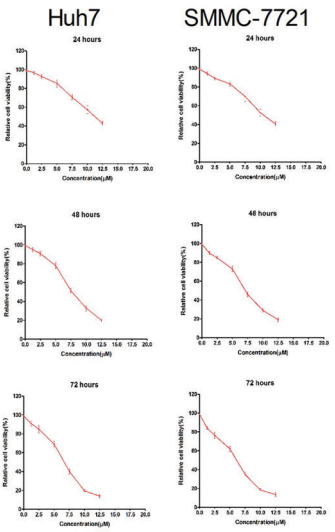

Sun and colleagues screened clustered regularly interspaced short palindromic repeats (CRISPR) to identify druggable genes associated with sorafenib-treated hepatocellular carcinoma (HCC). Of 19,050 genes tested, the knockout screen identified inhibition of SGOL1 expression as the most effective genetic suppressor of sorafenib activity; SGOL1 was thus an indicator of prognosis or of patients treated with sorafenib.

SGOL1 plays an established role in mitosis, with controversial roles in carcinogenesis and drug resistance. A total of 210 patients with HCC after hepatic resection were assessed for SGOL1 expression, and those with high expression showed significantly shortened overall survival. In the lab, loss of SGOL1 from HCC cells decreased the cytotoxicity of sorafenib, reducing apoptosis following treatment. The identification of this target suggests that the same screening protocol could be used to identify therapeutic targets of interest for other disease–drug outcomes.

TSG-6 attenuates intervertebral disc degeneration

doi:10.1038/s41374-018-0036-5

TNF-α-stimulated gene 6 protein (TSG-6) secreted by bone marrow mesenchymal stem cells (BMSCs) inhibits inflammatory processes in a variety of diseases. To investigate whether BMSCs exert this therapeutic effect in intervertebral disc degeneration by secreting TSG-6, Yang et al. developed a surgical model in rats. BMSCs and TSG-6 reduced the expression of MMP-3 and MMP-13 and increased expression of collagen II and aggrecan in IL-1β-treated nucleus pulposus cells (NPCs)—helpful effects that were attenuated when TSG-6 expression was silenced. Levels of IL-6 and TNF-α in degenerated NPCs were higher in the surgical group but were reduced with BMSC transplantation and TSG-6 expression intact. Treated NPCs were increased in the presence of BMSCs and TSG-6 mediated by decreased TLR2/NF-κB signaling, resulting in reduced expression of MMPs and inflammatory cytokines in degenerated NP tissues. The authors conclude that BMSC transplantation might delay, or even prevent, disc degeneration through TSG-6-mediated anti-inflammatory effects.

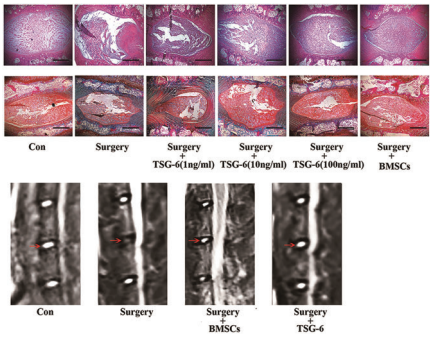

nature.com/pathology

Diversity of the noncoding genome

To investigate the noncoding human genome, di Iulio et al. assessed 11,257 whole-genome sequences and 16,384 heptamers to build a new map of sequence constraints in humans. In the most constrained genomic regions they identified regulatory elements that associate with the most essential genes. They also assessed constrained regions using a context-dependent tolerance score (CDTS) and genomic evolutionary rate profiling across 34 mammalian species; the results indicated that the CDTS can be used to identify these constrained regions. Essentiality scores (pLI score) were assigned to each genomic bin within 15 kb of a gene. Plotting against the CDTS showed a clear association between the essentiality of the associated gene and the CDTS of the distal regulatory element up to 2 Mb. Practically, this could allow targeting of sequencing efforts beyond the exome to include the cis or distal rare variants that regulate the expression of medically important genes.

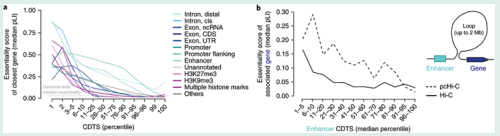

Nature Genetics 2018;50:333–337; doi:10.1038/s41588-018-0062-7

Maternal mutational clusters in oocyte aging

Whole-genome sequencing of 1,291 parent–offspring trios of average health at a single hospital revealed 1,796 clustered de novo mutations (cDNMs). cDNMs were defined as DNMs within the same individual with all pairwise intermutational distances smaller than 20 kb. Read phasing was used to identify the parent of origin of 700 cDNMs across 400 clusters, and a linear-regression model correlated parental age with the number of cDNMs in the offspring. Clusters were more prevalent on the maternal allele, and positively correlated with maternal age as compared with paternal clusters. More than 50% of maternal clusters were located on chromosomes 8, 9, and 16, with a distinct mutation signature of C>G transversions associated with double-strand breaks. High recombination rates in aging oocytes is suggested to provide protection against aneuploidy, and these clustered mutations seem to be selected for in conjunction with that protection.

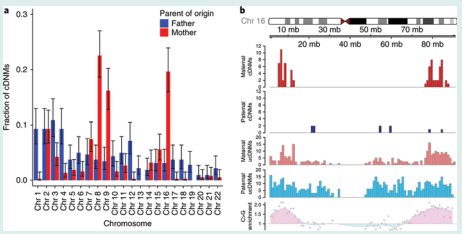

Nature Genetics 2018;50:487–492; doi:10.1038/s41588-018-0071-6

New oncogenic drivers in prostate cancer

Exome sequencing of 1,013 prostate cancers was performed to seek recurrently mutated genes at lower frequencies than those previously established. The group identified and validated a new class of E26 transformation–specific (ETS)–fusion–negative tumors, defined by mutations in epigenetic regulators and the spliceosome pathway. Given the increased detection power of this cohort, additional significantly mutated genes (SMGs) were noted in prostate cancer with incidences below 3% of cases. These results support the authors' contention of a long tail of SMGs in prostate cancer. Genes enriched in metastatic samples included *TP53*, *AR*, *PTEN*, *RB1*, *FOXA1*, *APC*, and *BRCA2*, with epigenetic regulators *KMT2C* and *KMT2D* also enriched in metastatic tumors, whereas SPOP was enriched in primary tumors. Among the next steps will be functional characterization of the relative phenotypic effects on oncogenicity, metastatic potential, and response characteristics to known or emerging prostate cancer therapeutics in order to use these data to influence prostate cancer therapeutics in the future.

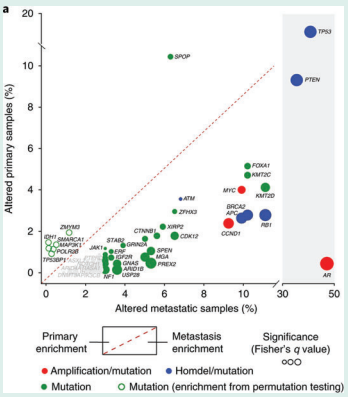

Nature Genetics published online 2 April 2018; doi:10.1038/s41588-018-0078-z

Emma Judson contributed to these reviews.